Test Structure for $I_C(V_{BE})$ Parameter Determination of Low Voltage Applications

W. Rahajandraibe[1], C. Dufaza[1], D. Auvergne[1], B. Cialdella[2], B. Majoux[2] and V. Chowdhury[2]
[1]LIRMM, UMR C5506 CNRS-Université de Montpellier II 161, rue Ada
34392 Montpellier Cedex 5, France
E-mail: {rahajan, dufaza, auvergne}@lirmm.fr
[2]ST-Microelectronics, 12, rue Jules Horowitz, B.P. 217 F-38019 Cedex, France
E-mail: {cialdella, majoux, chowdhury}@st.com

Abstract

The temperature dependence of the $I_C(V_{BE})$ relationship can be characterised by two parameters: E_G and X_{TI}. The classical method to extract these parameters consists in a "best fitting" from measured $V_{BE}(T)$ values, using least square algorithm at constant collector current. This method involves an accurate measurement of V_{BE} voltage and an accurate value of the operating temperature. We propose in this paper, a configurable test structure dedicated to the extraction of temperature dependence of $I_C(V_{BE})$ characteristic for BJT designed with bipolar or BiCMOS processes. This allows a direct measurement of die temperature and consequently an accurate measurement of $V_{BE}(T)$. First, the classical extraction method is explained. Then, the implementation techniques of the new method are discussed, the improvement of the design is presented.

1. Introduction

Due to the considerable expansion of portable applications like cellular telephone, PALM, electronic organiser and others, great interest is given to design methodologies for low consumption. As a consequence, we observe a continuous decrease of the values of the bias current and the supply voltage used in mixed integrated applications. Due to their very low consumption and their wide temperature range of operation, bandgap references are widely used in various types of analog circuits for signal processing such as A/D and D/A converters, voltage regulators and a number of measurement devices. Designing high stability circuits such as bandgap references demands to obtain a very good correlation between the physical parameters and their representation model used in electrical simulations. Characterising these parameters for low voltage and current operating points over a wide range of temperature is out of the current foundry measurement protocols. At low operating bias conditions parasitic effects are exhausted, this greatly modify the stability conditions at high temperature of critical designs such as bandgap references. This stability may be deduced from the BJT's saturation current equation commonly used in the electrical simulators [1]

$$I_S(T) = I_S(T_0)\left(\frac{T}{T_0}\right)^{X_{TI}} e^{-\frac{qE_G}{k}\left(\frac{1}{T}-\frac{1}{T_0}\right)} \qquad (1)$$

where q is the electron charge, k is the Boltzman constant and E_G is the forbidden energy band value at 0K of silicon, including bandgap narrowing, X_{TI} is a constant parameter, related to the temperature dependence of the mobility of minority carriers in the base region and T_0 is the reference temperature.

E_G and X_{TI} are among the most difficult parameters to be extracted or estimated. This is due to several reasons. Firstly due to impurity bandgap narrowing effects, it is very difficult to estimate the real value of E_G at 0K. In modern bipolar processes, the emitter doping profile has a very high peak value resulting in a decrease of the bandgap energy by about 45meV [2] for the Si devices and in the order of 150meV for the SiGe HBT's. Thus, this reduction must be included in the model. Secondly, due to the correlation between E_G and X_{TI} it is not possible to extract these parameters separately.

We propose in this paper, a test structure based on bandgap reference voltage that allows a more accurate extraction of E_G and X_{TI} parameter values by a direct measurement of the circuit operating temperature and therefore, a performance improvement of the same design. In part 2 we discuss the difficulties encountered in determining accurately the E_G value. The extraction method for E_G and X_{TI} parameters is proposed in part 3. In part 4 we detail the proposed implemented method and discuss the experimental results in part 5. We give the improvement possibility of the circuit in part 6 before to conclude in part 7.

2. Si bandgap energy determination

In order to determine the theoretical expression of parameters E_G and X_{TI} used in the simulation model according to (1), the equation of $I_S(T)$ obtained in the

Gummel-Poon model [1] is recapitulated in this section. It can be written as

$$I_S(T) = \frac{qA_e n_i^{\,2}(T)}{\int_{W_{bem}}^{W_{bcol}} \frac{N_{ab}(x,T)}{D_{nb}(x,T)} e^{-\frac{\Delta E_{Gbgn}(x)}{kT}} dx} \approx \frac{qA_e n_{ie}^{\,2}(T) D_{nb}(T)}{\int_{W_{bem}}^{W_{bcol}} N_{ab}(x,T)dx} \quad (2)$$

where A_e is the emitter area, n_i is the intrinsic carrier concentration, $D_{nb}(T)$ is the mean diffusion constant of electron in the base region, $N_{ab}(x,T)$ is the impurity doping in the base, ΔE_{Gbgn} represents the decrease of the bandgap of silicon due to high level impurity doping. W_{bem} and W_{bcol} are the limit of the neutral base from emitter and collector at zero biasing and $n_{ie}(T)$ represents the effective doping profile of intrinsic carriers given by

$$n_{ie}^{\,2}(T) = n_i^{\,2}(T) \times e^{\frac{\Delta E_{Gbgn}}{kT}} \quad (3)$$

Using the Einstein relation [3] and the mobility temperature variation, the mean diffusion constant D_{nb} can be written as

$$D_{nb}(T) = D_{nb}(T_0)\left(\frac{T}{T_0}\right)^{1-E_N} \quad (4)$$

where E_N is the temperature exponent. The temperature variation of the Gummel number can be written as

$$\int_{W_{bem}}^{W_{bcol}} N_{ab}(x,T)dx = N_G(T_0)\left(\frac{T}{T_0}\right)^{E\rho} \quad (5)$$

where E_ρ is the temperature exponent for the Gummel number. According to the Boltzman theory, n_i is given by

$$n_i^{\,2}(T) = n_i^{\,2}(T_0)\left(\frac{T}{T_0}\right)^3 e^{-\left(\frac{E_G(T)}{kT} - \frac{E_G(T_0)}{kT_0}\right)} \quad (6)$$

The values of E_G and X_{TI} of (1) can be obtained from physical experiments. However it appears [2], [4-5], that using values derived from solid state physics to design critical devices such as bandgap reference voltages, does not allow a satisfactory agreement between simulations and experiments. This discrepancy is shown to be mostly due to the approximation made for $E_G(T)$ in (6), which for many applications, is assumed to be linear. The equation of the temperature sensitivity of the energy band gap according to this assumption results in

$$E_G(T) = E_G(0) - aT \quad (7)$$

For high accuracy applications this model turns out to be unsatisfactory. More accurate model is defined [8] as

$$E_G(T) = E_G(0) + \frac{\alpha T^2}{T+\beta} \quad (8)$$

However, as shown in [6], (1) can not be justified from (8) and (6). To solve this problem, another model [7] of $E_G(T)$ was developed as

$$E_G(T) = E_G(0) + aT + bT\ln T \quad (9)$$

The equation of $n_{ie}(T)$ using this expression with (3) and the expression of $n_i(T)$, as defined in (6) gives

$$n_{ie}^{\,2}(T) = n_{ie}^{\,2}(T_0)\left(\frac{T}{T_0}\right)^{\left(3-\frac{b}{k}\right)} e^{-\frac{(E_G(0)-\Delta E_G bgn)}{k}\left(\frac{1}{T}-\frac{1}{T_0}\right)} \quad (10)$$

using (2), (4), (6) and (10) we obtain finally

$$I_S(T) = I_S(T_0)\left(\frac{T}{T_0}\right)^{\left(4-E_N-E_\rho-\frac{b}{k}\right)} e^{-\frac{(E_G(0)-\Delta E_G bgn)}{k}\left(\frac{1}{T}-\frac{1}{T_0}\right)} \quad (11)$$

By identifying this equation with (1), which is used to model the temperature variation of the saturation current in electrical simulation, results in

$$\begin{aligned} E_G &= E_G(0) - \Delta E_{Gbgn} \\ X_{TI} &= 4 - E_N - E_\rho - \frac{b}{k} \end{aligned} \quad (12)$$

where E_G and X_{TI} are the parameters used in SPICE to model the temperature variation of $I_C(V_{BE})$ characteristic for a BJT. In Fig. 1 we give the different models according to (7), (8) and (9) in which the different curves represent:

1. $E_{G1}(T)$ the linearized model (7) of $E_{G5}(T)$ from the chosen reference temperature,
2. $E_{G2}(T)$, the value obtained with (8) and $\alpha=7.021\times10^{-4}$ V/K, $\beta=1108$K and $E_{G2}(0)=1.1557$eV [8],
3. $E_{G3}(T)$, the related model to (8) and $\alpha=4.73\times10^{-4}$V/K, $\beta=636$K and $E_{G3}(0)=1.170$eV [7],
4. $E_{G4}(T)$, that corresponds to (9) and $E_{G4}(0)=1,1663$V, $a=6.141\times10^{-4}$V.K^{-1} $b=-1.307\times10^{-4}$ [6],
5. $E_{G5}(T)$, that corresponds to (9) and $E_{G5}(0)=1.1774$V, $a=3.042.10^{-4}$V×K^{-1} and $b=-8.459\times10^{-5}$ [6].

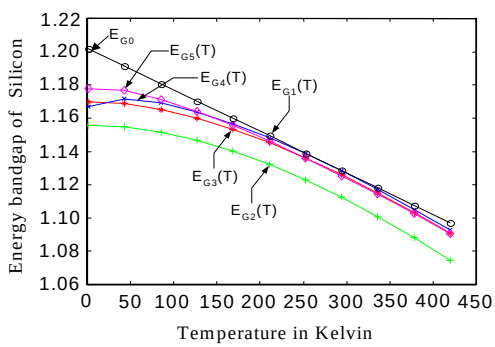

Fig. 1. Illustration of the different modelling of the temperature variation of the Si energy band gap.

As show in Fig. 1 there is no accordance in the values of bangap at 0K predicted by each model. The discrepancy between the $E_{G5}(0)$ and $E_{G2}(0)$ is about 22mV. This corresponds to the range of accuracy in low voltage design of bandgap references. This discrepancy is magnified assuming the extrapolated value of $E_{G5}(T)$ at the absolute zero temperature, E_{G0}. Furthermore, by considering the bandgap narrowing effect, the error introduced by this assumption may rise up to 90mV. Since more and more

bandgap reference voltages operate down to 600mV [9-11], it is clear that the performance improvement of low consumption circuits implies a more accurate determination of this parameter. Thus, not only an accurate model is required for the ultra low voltage, low consumption applications but also a good extraction strategy of the physical parameters on the process of integration and at the circuit working conditions.

3. Extraction method of E_G and X_{TI}

The relations given in (12) need a determination of E_N, $E\rho$, b, $E_G(0)$ and ΔE_{Gbgn}. In practice it is preferable to obtain directly E_G and X_{TI} from measurement techniques without a definition of the previous parameters. Several methods have been proposed to extract the temperature coefficients of the forward transport saturation current. One uses directly the $I_S(T)$ characteristic data. However, this method is not accurate because I_S does not come from direct measurements but from linear regressions. It is shown [12] that the sensitivity of I_S with temperature is very important, around 20% per degree. Another results from a fit on $V_{BE}(T)$ at low collector current value which is more accurate because $V_{BE}(T)$ is processed from direct measurements. Its expression can be written as

$$V_{BE}(T) = V_{BE}(T_0)\frac{T}{T_0}\left(\frac{V_{AR}-V_T(T_0)}{V_{AR}-V_T(T)}\right)+ \frac{V_{AR}}{V_{AR}-V_T(T)}\left[V_T(T)\ln\frac{I_C(T)}{I_C(T_0)}+V_T(T)X_{TI}\ln\frac{T_0}{T}+\frac{E_G}{q}\left(1-\frac{T}{T_0}\right)\right] \quad (13)$$

If V_{AR} and $V_{BE}(T_0)$ are known, E_G and X_{TI} can be determined directly from $V_{BE}(T)$ using least square fit without iteration. The accuracy of the precedent extraction method depends directly on the accuracy achievable on the measurement of $V_{BE}(T)$ characteristic. In other terms, it depends not only on the voltage measurement but also on the accuracy of the temperature determination. In addition to long measurement time we can show easily that a measurement error of 1% on the $V_{BE}(T)$ characteristic may induce up to 8% of error on the extracted values of E_G.

The proposed solution, described below, is based on a programmable configuration test cell implemented on a bandgap reference circuit. It allows an extraction of E_G and X_{TI} by measuring only a single temperature. It can be performed using Meijer equations [13] that principle is illustrated in the Fig. 2. Forcing identical collector currents for Q_A and Q_B, that area ratio is more than unity, makes their built-in voltage directly proportional to absolute temperature. Standard calculation using $I_C(V_{BE})$ characteristic results in

$$T_2V_{BE}(T_1)-T_1V_{BE}(T_2)=(T_2-T_1)E_G+X_{TI}\frac{kT_1T_2}{q}\ln\frac{T_2}{T_1} \quad (14)$$

$$T_3V_{BE}(T_2)-T_2V_{BE}(T_3)=(T_3-T_2)E_G+X_{TI}\frac{kT_2T_3}{q}\ln\frac{T_3}{T_2} \quad (15)$$

From the above equations, we obtain

$$T_1=\frac{\Delta V_{BE}(T_1)}{\Delta V_{BE}(T_2)}T_2 \text{ and } T_3=\frac{\Delta V_{BE}(T_3)}{\Delta V_{BE}(T_2)}T_2 \quad (16)$$

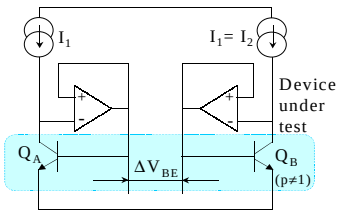

Fig. 2. Bias of BJT's under test for the temperature measurement using (16).

Knowing T_1, T_2, T_3, $V_{BE}(T_1)$, $V_{BE}(T_2)$ and $V_{BE}(T_3)$, E_G and X_{TI} can be extracted directly from (14) and (15). Then, only the temperature T_2 has to be measured. It is shown [13] that an error ΔT_2 less than 5°K has no significant influence on the calculated values of E_G and X_{TI}. With this configuration T_1 and T_3 are the real operating temperatures of the circuit.

4. Implementation of the method on silicon

In the industrial context, processes are characterised for a wide range of applications. Usually, the same model card is used to simulate several types of circuit that do not operate necessarily at the same bias level, either for low current applications or power applications. In our case, a number of bandgap test cells have been implemented in a ST-Microelectronics BiCMOS process, as shown in Fig. 3. Using a "standard SPICE model card" to simulate the temperature variation of V_{REF} for the present bandgap reference gives allure close to the curve *(S0)* as shown in the Fig. 8.

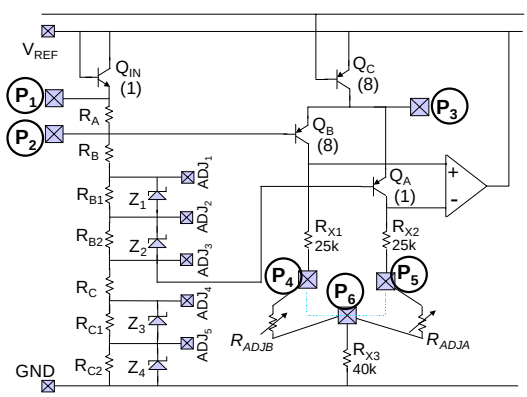

Fig. 3. Schematic of the programmable configuration test cell implemented in a bandgap circuit core.

However, measurements performed on the circuit implemented on silicon, in the temperature range extending from –50°C to 100°C, point out another temperature behaviour as shown (in •) in Fig. 8. Since E_G and X_{TI} appear directly in the voltage reference equation, a worth determination of these parameters induces direct error on the prediction of $V_{REF}(T)$ characteristic.

This extraction method can be processed using only a pair of transistors biased at a constant collector. However, in order to obtain the working temperature of the device to be modelled, we have implemented the test cell in a programmable configuration of bandgap reference voltage circuit. In this case, parameter extraction can be performed in biasing the BJT's under test at the same level than that of the bandgap reference. Second order effects such as self heating of the component under test, the offset of op amp stage, the effects related to packaging such as pressure, and other physical parameters can be taken into account in the model.

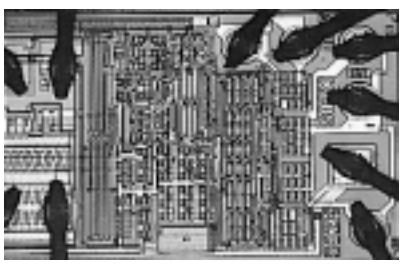

Fig. 4. Photograph of the complete bandgap circuit, including the implemented test cell, in the border is shown the access pads.

The method has been implemented on a PNP transistor pairs with an emitter area ratio of 8 (6µm², 48µm²), the BJT's are implemented in a BiCMOS process using a 3µm thick 0.8Ω-cm n-epitaxial layer, 2.5µm deep 21Ω/□ base diffusion. The resistors have been implemented in an n-well diffusion with 2kΩ/□. The photograph of the circuit is shown in Fig. 4. V_{REF} is directly measured at the base of Q_{IN}. The reference voltage is obtained by adding the built-in voltage of Q_{IN} to the VPTAT generated by the difference between the V_{BE} of Q_A and that of Q_B. The adjustment pads ADJ are used to correct the offset voltage of V_{REF} due to process spreading. Other access pads have been added in order to modify the configuration of the circuit on chip, in particular the saturation level of the device under test. Q_C ensures the bias of BJT's Q_A and Q_B. Fixing the same potential through R_{X1} and R_{X2} imposes the equality between the collector current of Q_A and Q_B. Due to the leakage current of the parasitic transistor of Q_B which is eight time larger than that of Q_A, the collector currents are not really identical, this effect is even more important when the BJT's work at the limit of the saturation. Pads P_4 and P_5 have been added in order to correct this effect and the offset of the amplification stage.

In practice, identical bias current for Q_A and Q_B must be ensured whatever the temperature level is. In other terms an external current source that is not influenced by the temperature variation should be used. The collector currents I_{CQA} and I_{CQB} increase with temperature. We can rewrite (14) and (15) by including I_{CQA} and I_{CQB} as

$$T_2V_{BE}(T_1)-T_1V_{BE}(T_2)=(T_2-T_1)E_G+X_{TI}\frac{kT_1T_2}{q}\ln\frac{T_2}{T_1}+\frac{kT_1T_2}{q}\ln\left(\frac{I_{C1}(T_1)}{I_{C1}(T_2)}\right) \quad (17)$$

$$T_2V_{BE}(T_1)-T_1V_{BE}(T_2)=(T_2-T_1)E_G+X_{TI}\frac{kT_1T_2}{q}\ln\frac{T_2}{T_1}+\frac{kT_1T_2}{q}\ln\left(\frac{I_{C2}(T_1)}{I_{C2}(T_2)}\right) \quad (18)$$

By re-evaluating the temperature equations we obtain

$$T_1=\Delta V_{BE}(T_1)\times\frac{1}{\Delta V_{BE}(T_2)+\frac{kT_2}{q}\ln(X)}\times T_2 \quad (19)$$

$$\text{with } X=\frac{I_{C1}(T_1)\times I_{C2}(T_2)}{I_{C1}(T_2)\times I_{C2}(T_1)} \quad (20)$$

Similar equation is obtained for T_3. If we evaluate the coefficient $A=\frac{kT_2}{q}\ln(X)$ for two temperatures T_1=0°C and T_2=100°C, we obtain A≈0.3mV (0.45% of $\Delta V_{BE}(T_2)$), for a variation $\Delta V_{BE}(T_2)$=70mV. This gives evidence that the temperature variation of I_C has a weak influence on the values of T_1 and T_2.

5. Experimental results

E_G and X_{TI} extractions have been performed with two different methods and the results have been compared. The first method consists in a best fitting on measured data of the $V_{BE}(T)$ characteristic processed on a single BJT. A complete set of resulting $I_C(V_{BE})$ characteristics from –50°C to 125°C is represented in Fig. 5.

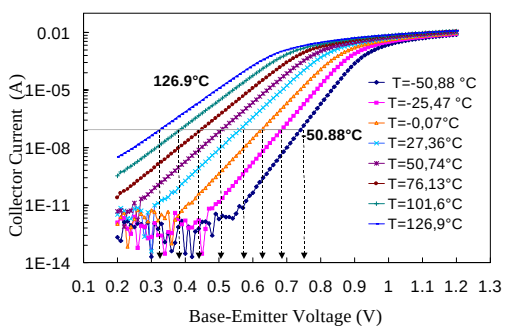

Fig. 5. Complete set of $I_C(V_{BE})$ characteristic for a BJT in the temperature range of –50°C to 125°C, measured by a step of 25°C.

Several $V_{BE}(T)$ characteristics at a fixed collector current can be extracted from this set. E_G and X_{TI} best fitting values have been obtained from a fit of (13) on the

complete set of $V_{BE}(T)$ characteristics measured on a range of current extending from $I_C=1\times10^{-8}$ to 1×10^{-5}A. This results in an infinite number E_G and X_{TI} couples, due to the correlation between these parameters. These couples of value form a straight line called "characteristic straight" as shown in Fig. 6. The second one is an analytical method using the solution of (14) and (15). The complete characteristic $V_{BE}(T)$ of the pair of transistors Q_A and Q_B has been measured directly on the biased test cell for a number of samples. The temperature sensor HP34970A with sonde pt100 4 wires and a precision less than 1°C is placed on the component. The ensemble of the devices: component-sensor is placed in a hermetic partition. Great care is given to insure that each point is measured in a complete thermal equilibrium. Voltage and current measurements have been performed with the HP4156 parameter analyser. The $V_{BE}(T)$ characteristic is measured between –50°C to 125°C by a step of 25°C. The reference temperature has been chosen at T_2=25°C. Data measured at the temperature T_1=-25°C and T_3=75°C have been used in (14) and (15) and have been compared to the data processed with the computed temperatures.

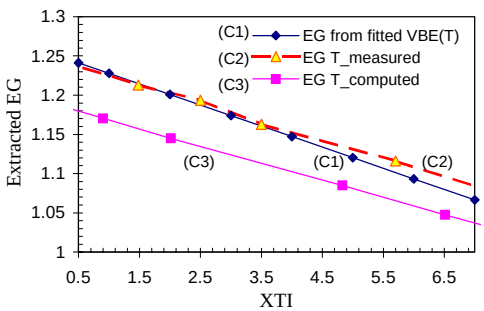

Fig. 6. "Characteristic straight " $E_G(X_{TI})$ extracted from the best fitting of $V_{BE}(T)$ and from analytical method with measured and computed temperature values.

Note that the $E_G(X_{TI})$ "characteristic straight", illustrated in Fig. 6 and derived from the best fitting method *(C1)* is in good correlation with that obtained with the analytical method *(C2)* by substituting the measured T_1 and T_3 into (14) and (15). This gives indication of the equivalence between these two methods. The temperature values used in these first extractions are both those given by the temperature sensor. However they are in poor agreement with the values computed from (16) that correspond to the real temperature of the BJT's under test. The third straight line *(C3)* is extracted using the analytical method by considering also T_2=25°C as a reference and computing the values of T_1 and T_3 from (16).

The difference between the measured and computed values of the temperatures T_1, T_2 and T_3 using the ΔV_{BE} of BJTs Q_A and Q_B is shown in Table 1 for five samples of the test cell. The measurement error at the reference temperature T_2=25°C is assumed to be negligible. The difference between the measured and the computed temperatures varies from –2°C to –5°C for T_1, and from 4°C to 7°C for T_3. In fact the slope of $V_{BE}(T)$ at 25°C is modified by about 8%, but this is enough to introduce a dramatic difference in the value of the extracted parameters. Assuming that the transistors Q_A and Q_B are correctly matched, the difference between the external and the die temperatures is due to the bias current of the circuit, and then to self-heating of Q_A, Q_B and the other components on the chip. This effect is pointed out by the analytical method.

	T_measured - T_computed (K)				
Measured temperature (K)	sample 1	sample 2	sample 3	sample 4	sample 5
T_1 = 247	-3.6	-4.53	-4.35	-4.61	-1.82
T_2 = 297	0	0	0	0	0
T_3 = 348	6.61	5.64	3.99	4.02	7.28

Table 1. Comparison of uncertainties in the temperature values obtained from the sensor and that computed from (16) for five samples of the bandgap test cell.

Couples belonging to each "characteristic straight" have been introduced in the model card to simulate the bandgap reference voltage. As shown in Fig. 8, there is a very good correlation between the measured value of $V_{REF}(T)$ performed on one sample of the circuit and that simulated with the model card in which the values of E_G, X_{TI} extracted from the analytical method have been used (curve *(S1)*). According to the $V_{REF}(T)$ characteristic (curve *(S0)*) predicted by the simulation with the model card, in which E_G and X_{TI} are extracted from the "best fitting" method, the $V_{REF}(T)$ allure seems to be close to a bell curve. This is the expected typical shape of the temperature variation of a bandgap reference voltage, which does not correspond to the variation measured on the circuit. Observing the discrepancy between the real and simulated values of $V_{REF}(T)$, using the best fitted parameters, demonstrates the difficulty in optimising the structures.

6. Improvement of the structure

The bandgap reference voltage is obtained by adding the base-emitter voltage of Q_{IN}, which is PTAT, and the ΔV_{BE} generated by the couple Q_A and Q_B which is CTAT (Complementary To Absolute Temperature). To obtain a CTAT voltage, the transistor Q_B is made eight times larger than Q_A. Because of the low voltage operating of the circuit, these components work in the saturation region, therefore their parasitic transistors introduce non-linear component in the generated ΔV_{BE}. This results to a dramatic rise of $V_{REF}(T)$ characteristic with the

temperature. Unfortunately this effect is not pointed out by the standard model card. The temperature behaviour of $V_{REF}(T)$ expected from the considered bandgap reference circuit matches the *(S0)* curve (Fig. 8) which is not that measured on the circuit (in •). Using the model card in which E_G and X_{TI} are extracted with the proposed test structure, the temperature stability of the design could be improved. Adjustment resistors R_{adjA} is added between P_5 and P_6 in order to correct the non linear component of ΔV_{BE} due to the substrate leakage current and the offset of op-amp stage. The simulated $V_{REF}(T)$ characteristic for some values of R_{adjA} is illustrated *(S1-S4)* in Fig. 8.

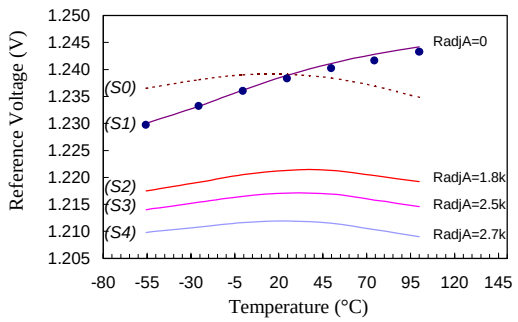

Fig. 8. Comparison between the temperature variation of the reference voltage measured on a sample of diffusion lots with the simulated variation of improved circuit.

It is clearly shown in this figure that with a good extraction strategy of the physical parameters, a better correlation between the simulation and the measurement can be performed. It has been done with a configurable test structure that gives a possibility to really improve the design.

7. Conclusion

Different extraction methods of the parameters related to the temperature variation of the saturation current of the BJT are presented, tested and discussed in this paper. The first one consists in a best fitting from $V_{BE}(T)$ characteristic. In this approach, a complete built-in voltage characteristic is needed. Therefore, perfect temperature matching between the temperature sensor and the device under test has to be achieved in order to minimise the extraction errors. In this case the measurements have been done with a single transistor. In addition to the long measurement time, second order effects could not be taken into account. Thus, a second approach has been proposed, which is based on an analytical method. This allows a direct measurement on the circuit implementation and needs only one temperature measurement. The technique is implemented in a programmable configuration test cell based on a bandgap reference voltage circuit. It is clearly shown that the parameters extracted from this new approach allow a very close matching with the temperature variations observed on a real bandgap reference voltage. In other terms, parameters extracted with this last method include the second order effects of the complete circuit which are impossible to reproduce using an extraction with a single component. The present test structure can be used to prototype the design of more accurate low voltage reference circuit.

References

[1] H.K. Gummel, H.C. Poon, "An Integral charge model of bipolar transistors," Bell Syst. Tech. J., vol. 49, pp. 827-851, 1970.

[2] P. Ashburn, H. Boussetta, M. D. R. Hashim, A. Chantre, M. Mouis, G. J. Parker, " Electrical determination of bandgap narrowing in bipolar transistors with epitaxial Si, epitaxial $Si_{1-X}Ge_X$, and ion implanted bases," *IEEE Trans Elect Devices*, vol. 43, n°5, pp. 774-783, May 1996.

[3] S.M. Sze, "Physics of Semiconductor Devices", 2nd edition, 1981 John Wiley & Sons, Inc.

[4] Y. P. Tsividis, "Accurate analysis of temperature effects in I_C-V_{BE} characteristics with application to bandgap reference sources," *IEEE J. Solid-State Circuits*, vol. SC-15, n°.6, pp. 1139-1143, Dec. 1980.

[5] K. E. Kuijk, "A precision reference voltage source," *IEEE J. Solid-State Circuits*, vol. SC-6, pp.222-226, June 1973.

[6] N. Gambetta, and D. Celi, "Simple and accurate method for determining E_G and X_{TI} SPICE parameters," *ST-microelectronics Central R&D, Modelling and Characterisation*, 1992.

[7] C. D. Thurmond, "The standard thermodynamic functions for the formation of electrons and holes in Ge, Si, GaAs, and GaP," *J. Electrochem. Soc. Solid-State Sci. And Technology*, vol. 122, no. 8, pp. 1133-1141, 1975.

[8] Y. P. Varshni, "Temperature dependence of the energy gap in semiconductors," *Physica*, vol. 34, pp. 149-154, 1967.

[9] G. A. Rincon-Mora and P. E. Allen, "A 1.1-V current-mode and piecewise-linear curvature-corrected bandgap reference," *IEEE J. Solid-State Circuits*, vol. 33, pp. 1551-1554, Oct. 1998.

[10] H. Banba, H. Shiga, A. Umezawa, T. Miyaba, T. Tanzawa, S. Atsumi and K. Sakui, "A CMOS bandgap reference circuit with sub-1-V operation," *IEEE J. Solid-State Circuits*, vol. 34, pp. 670-673. May 1999.

[11] A-J. Annema, "Low-power bandgap referencrs featuring DTMOST's," *IEEE J. Solid-State Circuits*, vol. 34, pp. 949-955, July 1999.

[12] R. U. Martinelli, "The temperature dependence of DC base and collector current in silicon bipolar transistors," *IEEE Trans. Elect. Devices*, pp. 1218-1224, Nov. 1976.

[13] Gerard C. M. Meijer and Kees Vingerling, "Measurement of temperature dependence of the $I_C(V_{BE})$ characteristics of integrated bipolar transistors," *IEEE J. Solid-State Circuits*, vol. SC-15, n°2, pp. 237-240, April 1980.